

Graphene as a metal passivation layer: Corrosion-accelerator and inhibitor



Mankyu Jo¹, Hyo Chan Lee¹, Seung Goo Lee, Kilwon Cho^{*}

Department of Chemical Engineering, Pohang University of Science and Technology, Pohang, 37673, South Korea

ARTICLE INFO

Article history:

Received 12 October 2016

Received in revised form

2 February 2017

Accepted 3 February 2017

Available online 5 February 2017

ABSTRACT

Despite the extraordinary impermeability of graphene, graphene fails to prevent oxidation of Cu surfaces under ambient conditions. Cu surfaces under a graphene layer oxidized faster than a bare Cu surfaces. The mechanism underlying the accelerated oxidation of Cu surfaces under graphene has remained unclear and has limited the application of graphene as an oxidation barrier for various metals. Here, we elucidated the mechanism underlying oxidation of a Cu surface under graphene layers. The diffusivity of Cu cation vacancies through the oxide layer, which is the rate-determining step of Cu oxidation, was found to be affected by a graphene layer via changes in the chemical composition of the oxide. Based on our findings, we proposed methods for improving the oxidative barrier properties of graphene. This work could provide guidance on the use of graphene to prevent oxidation of various metals.

© 2017 Published by Elsevier Ltd.

1. Introduction

Metal oxidation is a critical problem because this process can degrade the properties of the metal, such as its electrical and thermal conductivity. Long-term uses of metals require the presence of oxidation barriers that exclude oxidants [1–3]. Graphene, a two-dimensional sp^2 carbon material, has many potential applications in various fields due to extraordinary properties such as single-atomic thickness, high thermal and electrical conductivity [4–10]. In particular, impermeability of graphene, excluding even single He atoms, makes graphene as a promising material for oxidation barrier [11–13]. It has been demonstrated that deposition of graphene on a Cu surface can effectively prevent Cu oxidation under harsh conditions, such as thermal [14–18] or electrochemical corrosive conditions [19–23].

However, previous evaluations of graphene as an oxidation barrier to Cu under ambient conditions have reached contradictory conclusions [24–28]. Two papers reported that as-grown graphene on Cu accelerated the oxidation of Cu under ambient conditions by providing an additional electrical path that led to the rapid formation of oxygen ions at the air/oxide interface [24,25]; another study where graphene was used reported that graphene effectively

prevented oxidation of Cu under ambient conditions [26]. These inconsistent results suggested that some critical parameters that determined the barrier properties of graphene under ambient conditions remained uncontrolled. Moreover, a lack of understanding of Cu oxidation in the presence of graphene under ambient conditions has limited the practical application of graphene as an oxidation barrier for Cu and other metals.

Here, we revealed oxidation mechanism of a Cu surface under a graphene in comparison to bare Cu under ambient conditions. In addition, we investigated the effects of defects in graphene on the oxidation of an underlying Cu surface. Finally, we investigated oxidation behaviors of Cu surfaces under transferred graphene.

2. Experimental section

2.1. Sample preparations

We prepared two types of Cu samples to investigate the effects of graphene on Cu oxidation under ambient conditions: bare Cu, the native oxide of which was eliminated by H_2 annealing at 1000 °C and graphene-covered Cu (G-Cu) where graphene was directly synthesized by conventional chemical vapor deposition method [29–31]. We prepared defect-controlled graphene-covered Cu using H-plasma treatment (40 W) to investigate the effect of graphene defects on Cu oxidation under ambient conditions. The defects of graphene were controlled by H-plasma time. Transferred graphene-covered Cu (TrG-Cu) was prepared by conventional wet

^{*} Corresponding author.

E-mail address: kwcho@postech.ac.kr (K. Cho).

¹ These authors equally contributed to this work.

graphene transfer which is assisted by polymethyl methacrylate on bare Cu [32]. Bare Cu, G-Cu and TrG-Cu surfaces were then exposed to air over 1 year (Temperature = 293 K, $P_{\text{water}} = 0.8$ kPa, $P_{\text{oxygen}} = 20$ kPa). Bare Cu and G-Cu were dipped in 80 °C water over 4 h for wet corrosion.

2.2. Characterization

The surface morphology of species was characterized by optical microscopy (Axioplan, Zeiss). Raman spectra and Raman maps were taken by Raman spectroscopy (Alpha300R, WITec) using a laser with 488 nm wavelength as the excitation source. The defect density (n_d) of graphene was calculated from Raman I_D/I_G ratio of graphene using the following equation [33], $\frac{I_D}{I_G} = \frac{160}{E_L^2} \frac{r_A^2 - r_S^2}{r_A^2 - 2r_S^2} [\exp(-\pi r_S^2/L_D^2) - \exp(-\pi(r_A^2 - r_S^2)/L_D^2)]$ where r_A is the radius of Raman active area, r_S is the radius of structurally disordered area, L_D is average distance between defects and E_L is the excitation energy. From the obtained L_D , defect density can be calculated by the following equation, $n_d(\text{cm}^{-2}) = 10^{14}/(\pi L_D^2(\text{nm}^2))$. Cross-sectional TEM specimens were prepared by focused ion beam system (Helios, FEI) and images were taken by JEM-2200FS with image Cs-corrector (JEOL) operated with 200 kV. Electron energy loss spectra maps were taken by electron energy loss spectrometer attached to JEM-2200FS. Energy-dispersive X-ray spectra were taken by energy-dispersive X-ray spectrometer attached to JEM-2200FS. X-ray photoelectron spectroscopy spectra were taken by X-ray photoelectron spectroscopy (ESCALAB 250Xi, Thermo Scientific) using monochromated Al K α source (1486.6 eV). XPS depth profiles were taken by combining Ar⁺ ion etching with X-ray photoelectron spectroscopy measurement. The Cu oxide thickness was estimated from the ratio between Cu₂O and CuO oxide peaks to metal Cu peaks intensity (I_0/I_m) in X-ray photoelectron spectra using the following Strohmeyer equation, $d_{ox} = \lambda_0 \ln \left(\frac{N_m \lambda_m I_0}{N_o \lambda_o I_m} + 1 \right)$ where the ratio of the volume density of bulk Cu to oxide (N_m/N_o) are 3.28 for Cu₂O and 1.75 for CuO, inelastic mean free path (λ_0) are 2.86 nm for Cu₂O, 2.80 nm for CuO, and 1.35 nm for Cu. The intensity ratio (I_0/I_m) is obtained from Cu LMM spectra for Cu₂O and Cu 2p spectra for CuO [34]. Electron backscattered diffraction maps were taken by electron backscattered diffraction detector attached to focused ion beam system (Helios, FEI).

3. Results and discussion

3.1. Long-term oxidation behaviors of G-Cu and bare Cu in ambient conditions

The oxidation behaviors of the bare Cu and G-Cu surfaces clearly differed (Fig. 1, Fig. S1). The surface of the as-prepared bare Cu was reddish-orange in color, which is characteristic of Cu. After exposure to air for 1 year, most Cu grains retained their reddish-orange color, but a few Cu grains changed from reddish-orange to pink (Fig. 1a); the rarity of this change indicated that the Cu surface was almost entirely passivated. In the case of G-Cu, the initial surface of the G-Cu was almost identical to that of the bare Cu. After exposure to air for 1 year, on the other hand, the color had changed to red, a characteristic color of Cu₂O, and reddish orange grains, which indicated severe oxidation of the Cu surface at particular grains (Fig. 1b, see also Figs. S1 and S2).

We investigated the correlation between the degree of oxidation and the crystallographic orientations of the G-Cu grains using the Raman peak of Cu oxide (near 639–652 cm⁻¹). To this end, a Raman spectroscopic map and an EBSD map at the same position

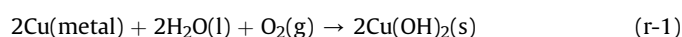
(250 $\mu\text{m} \times 250 \mu\text{m}$) on the G-Cu sample were obtained (Fig. S2). The intensity of the Raman peak of Cu oxide strongly depended on the misorientation angle of the Cu surfaces from Cu(100) (Fig. 1c). The Cu(100) surface was harshly oxidized, and the degree of oxidation of the Cu surface was reduced as the misorientation angle from Cu(100) increased. To investigate relevant factors that contributed to this dependence, we examined the quality of the graphene layer formed on Cu grains of different crystallographic orientations (Fig. 1d). The I_D/I_G ratio of graphene, which provided information about defect density of graphene [33], was independent of the crystallographic orientation of the Cu surface. This observation indicated that the dependence of the oxidation behavior on the crystallographic orientations of the underlying Cu surface was not related to the quality of graphene on the Cu surfaces with different crystallographic orientations. The mechanism underlying the orientation-dependent Cu oxidation of G-Cu in detail is discussed in Fig. S2.

A Raman spectroscopic analysis (Fig. 1e) confirmed that the bare Cu and G-Cu surfaces had reached different oxidation states after 1 year. The Raman spectrum of bare Cu after 1 year was relatively featureless, but the Raman spectrum of G-Cu after 1 year revealed distinct strong Raman peaks at 109, 154, 218, 308, 436, 515, 635, 665 and 820 cm⁻¹ that were characteristic peaks of Cu oxide [25]. As shown in Fig. 1f, I_{2D}/I_G ratio in Raman spectrum of as-prepared G-Cu indicated the synthesized graphene was single-layer graphene [29]. The negligible change in Raman spectra of G-Cu indicated that graphene was negligibly oxidized. X-ray Photoelectron Spectroscopy (XPS) C 1s spectrum of 1 year aged graphene also confirms that graphene was stable to oxidation at ambient conditions (Fig. S3). It shows accelerated Cu oxidation under graphene is irrelevant to degradation of graphene.

For direct comparison of the oxide thicknesses, cross-sectional high-resolution transmission electron microscopy (HR-TEM) images of the 1 year aged bare Cu and G-Cu and corresponding electron energy loss spectroscopy (EELS) oxygen maps were obtained (Fig. 2). For bare Cu, about 5 nm thick oxide layer had formed after 1 year of exposure to air (Fig. 2a). On the other hand, the thickness of the Cu oxide layer under graphene exceeded 10 nm (Fig. 2b). As shown in EELS maps, the oxygen concentration was abruptly reduced at oxide/Cu interface for both cases, indicating internal oxide growth was absent and only external oxidation occurred. Additionally, atomic ratios of the oxides obtained by Energy-dispersive X-ray spectroscopy (EDS) in TEM show that the oxide compositions of bare Cu and G-Cu are CuO and Cu₂O, respectively (Fig. S4).

We next examined the chemical composition of the oxide layers using XPS (Fig. 3). Cu LMM (Fig. 3a) and Cu 2p (Fig. 3b) spectra were collected from bare Cu (bottom) and G-Cu (top). The Cu LMM spectra show two characteristic peaks at 568.2 eV and 570.3 eV, mostly representing Cu metal and Cu₂O, respectively, and 3 other peaks originating from different transition states [34–36]. Both the bare Cu and G-Cu surfaces had the Cu₂O peak at 570.3 eV in both Cu LMM spectra (Fig. 3a). The Cu 2p spectra show 3 distinctive peaks at 932.5, 933.8, and 935.1 eV, which correspond to Cu metal and Cu₂O, CuO, and Cu(OH)₂, respectively [34–36]. The CuO peak (933.8 eV) and Cu(OH)₂ peak (935.1 eV) were clearly observed on the bare Cu surface. By contrast, only a single peak at 932.5 eV was observed on the G-Cu surface (Fig. 3b).

When Cu is oxidized at room temperature, the formation of CuO is determined by the presence of H₂O. When water layer wets Cu surface, CuO can be formed by following electrochemical reactions [34],



Download English Version:

<https://daneshyari.com/en/article/5432178>

Download Persian Version:

<https://daneshyari.com/article/5432178>

[Daneshyari.com](https://daneshyari.com)